

Chemical Science

Accepted Manuscript



This article can be cited before page numbers have been issued, to do this please use: M. K. Wong, J. Deng, W. Chan, N. C. Lai, B. Yang, C. Tsang, B. C. Ko and S. L. Chan, *Chem. Sci.*, 2017, DOI: 10.1039/C7SC02294H.



This is an Accepted Manuscript, which has been through the Royal Society of Chemistry peer review process and has been accepted for publication.

Accepted Manuscripts are published online shortly after acceptance, before technical editing, formatting and proof reading. Using this free service, authors can make their results available to the community, in citable form, before we publish the edited article. We will replace this Accepted Manuscript with the edited and formatted Advance Article as soon as it is available.

You can find more information about Accepted Manuscripts in the [author guidelines](#).

Please note that technical editing may introduce minor changes to the text and/or graphics, which may alter content. The journal's standard [Terms & Conditions](#) and the ethical guidelines, outlined in our [author and reviewer resource centre](#), still apply. In no event shall the Royal Society of Chemistry be held responsible for any errors or omissions in this Accepted Manuscript or any consequences arising from the use of any information it contains.

Photosensitizer-free visible light-mediated gold-catalysed *cis*-difunctionalization of silyl-substituted alkynes

Jie-Ren Deng,^{ab} Wing-Cheung Chan,^b Nathanael Chun-Him Lai,^{ab} Bin Yang,^{ab} Chui-Shan Tsang,^b Ben Chi-Bun Ko,^{b†} Sharon Lai-Fung Chan,^{ab†} and Man-Kin Wong^{*ab}

Received 00th January 20xx,
Accepted 00th January 20xx

DOI: 10.1039/x0xx00000x

www.rsc.org/

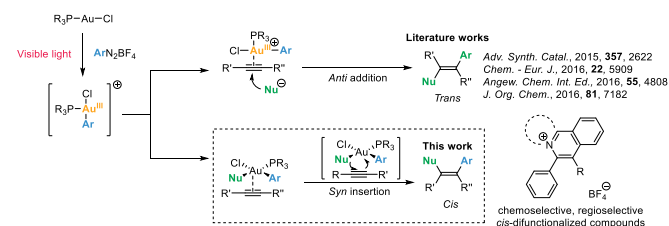
A new photosensitizer-free visible light-mediated gold-catalysed *cis*-difunctionalization reaction is developed. The reaction was chemoselective towards silyl-substituted alkynes with excellent regioselectivity and good functional group compatibility, giving a series of silyl-substituted quinolizinium derivatives as products. The newly synthesized fluorescent quinolizinium compounds, named JR-Fluor-1, possessed tunable emission properties and large Stokes shifts. With unique photophysical properties, the fluorophores have been applied in photooxidative amidations as efficient photocatalysts and cellular imaging with switchable subcellular localization properties.

Introduction

Over the past years, homogeneous gold catalysis has become a powerful tool for synthesis of complex organic molecules, particularly in activation of C–C multiple bonds with gold catalysts acting as strong soft π -Lewis acids.¹ In recent years, instead of accessing hydrofunctionalized products, a promising cross-coupling strategy involving Au(I)/Au(III) catalytic cycles has been developed to afford difunctionalized products.² With a significantly high redox potential of Au(I)/Au(III) couple, strong oxidants are required to access the oxidation of Au(I) species, while the functional group compatibility could be hampered.^{3a} A complementary approach to overcome this barrier was developed by Glorius³ and Toste⁴ through merging gold catalysis with photoredox catalysis, which promoted oxidation of Au(I) species employing photosensitizers and aryl radicals generated *in situ* under irradiation. This approach inspired the development of diverse organic transformations including difunctionalization of alkenes,^{3b-c,4b} allenes^{5a} and alkynes,^{3e,5b-c} as well as C–C^{3d,4d,5d-f} and C–P^{4c} cross-coupling reactions. Recently, Hashmi and co-workers reported visible light-mediated gold-catalysed oxyarylation of alkynes^{6a} and aryl-aryl coupling reaction^{6b} which could be conducted without addition of photosensitizers.

For alkyne difunctionalization reactions, undergoing an *anti* nucleophilic addition, *trans*-difunctionalized products are

afforded in the majority of the examples.^{3c,e,5c,6a} However, visible light-mediated *cis*-difunctionalization of alkynes still remains largely unexplored.⁷ Inspired by a stereo- and regioselective gold-catalysed hydroamination of internal alkynes reported by Stradiotto *et al.*,⁸ we set out to combine visible light mediated Au(I)/Au(III) catalysis with plausible *syn* insertion pathway to achieve alkyne *cis*-difunctionalization products.^{7b-c}



Scheme 1 Literature works and our strategy for visible light-mediated gold-catalysed alkyne *cis*-difunctionalization.

Development of organic fluorescent materials has become an emerging and important research area due to their wide applications in chemistry, biology and materials science.⁹ Compared to the intensive investigations on scaffolds such as fluorescein, BODIPY and recently Seoul-Fluor,¹⁰ only a few examples of cationic fluorophores have been reported, although the unique properties of fluorophores containing positive charge have been demonstrated in photocatalysis and cellular imaging.¹¹ Quinoliziniums, cationic aromatic heterocycles bearing quaternary bridgehead nitrogen, were firstly investigated in alkaloids chemistry and recently employed as efficient DNA intercalators.¹² However, structure photophysical property relationship (SPPR) studies and applications in photocatalysis and cellular imaging of quinolizinium compounds still remain elusive.¹³

Along with our ongoing interest in gold-catalysed organic transformations,¹⁴ herein, we report a new photosensitizer-free visible light-mediated gold-catalysed alkyne *cis*-difunctionalization

^a The Hong Kong Polytechnic University Shenzhen Research Institute, Shenzhen, People's Republic of China

^b State Key Laboratory of Chirosciences and Department of Applied Biology and Chemical Technology, The Hong Kong Polytechnic University, Hung Hum, Hong Kong

[†] Dr. Sharon Lai-Fung Chan designed and performed the spectroscopic studies and computational experiments of this research. Dr. Ben Chi-Bun Ko designed the cellular imaging experiments.

Electronic Supplementary Information (ESI) available: [details of any supplementary information available should be included here]. See DOI: 10.1039/x0xx00000x



tion reaction affording a series of silyl-substituted fluorescent quinolizinium compounds. Spectroscopy experiments and DFT calculations were conducted to study the SPFR of the quinolizinium derivatives. Applications of the fluorescent quinolizinium compounds as efficient photocatalysts for photooxidative amidation and as fluorescent dyes for live cell imaging have also been conducted.

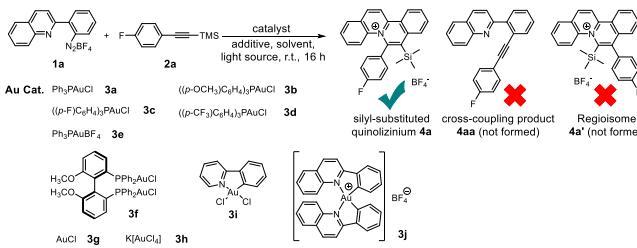
Results and discussion

We initiated the reaction screening by treatment of quinoline-substituted aryl diazonium **1a** (0.12 mmol, 1.2 equiv.), (4-fluorophenylethynyl)trimethylsilane **2a** (0.10 mmol, 1 equiv.) with Ph_3PAuCl **3a** (10 mol%) to afford silyl-substituted quinolizinium **4a** in 71% yield (Table 1, entry 1). To our surprise, no cross-coupling product **4aa** (reported by Toste *et al.* using phenyl diazoniums as substrates) was obtained in our experiments.^{4d} Besides, the reaction was exceptionally regioselective giving no regioisomer **4a'**. The gold(I) catalyst **3b** bearing comparatively electron-rich phosphine led to a lower yield of product formation, while catalysts **3c-d** bearing electron-poor phosphine gave higher yields of **4a** (entries 3-4). No desired product was obtained when $\text{Ph}_3\text{PAuBF}_4$ **3e** was employed as catalyst (entry 5). Using gold(I) catalyst **3f** possessing diphosphine ligand led to product formation in 21% yield (entry 6). Only a trace amount of product was observed when simple AuCl **3g** was used (entry 7). In addition, employing gold(III) catalysts **3h-j** resulted in no product formation (entries 8-10). Without addition of gold catalyst, no desired product was observed (entry 11), indicating that the gold(I) phosphine chloride catalyst played a crucial role in this transformation. Addition of transition metal-based photocatalysts $\text{Ru}(\text{bpy})_3\text{Cl}_2$, $\text{Ru}(\text{bpy})_3(\text{BF}_4)_2$, $\text{Ir}(\text{ppy})_3$ or organic photocatalyst Rose Bengal led to lower yields of the desired product (entries 12-15). Control experiment in dark gave no product formation (entry 16). These results suggested that this reaction was conducted under photosensitizer-free reaction conditions. Additionally, only a trace amount of product was detected when the reaction was conducted in toluene, dichloromethane or methanol as solvent (entries 17-19), and a lower yield (35%) of product was afforded when the reaction was carried in open air (entry 20).

With the optimized reaction conditions, we expanded the scope of this reaction by using various diazoniums (0.60 mmol, 1.2 equiv.) and alkynes (0.50 mmol, 1.0 equiv.) as substrates. Silyl-substituted alkynes **2a-q** bearing ether, alkyl, halogen, aldehyde, carboxylic acid, cyanide, trifluoromethyl, nitro and hetero-aromatics as substituents were well tolerated with the reactions giving quinolizinium products **4a-q** in 31-69% yield. Increasing the steric bulkiness using *ortho*-disubstituted phenylethynylsilane **2r** gave a trace amount of product. Using triethylsilyl group gave quinolizinium **4u** in slightly lower yield (45%). Further increasing the bulkiness employing *tert*-butyldiphenylsilyl-substituted alkyne **2t** gave no product **4v**. Interestingly, employing terminal alkyne phenylacetylene **2u**, cyclohexylacetylene **2v** or internal alkyne 1,2-diphenylethyne **2w**, 1-phenyl-1-propyne **2x**, 1-phenyl-1-butyne **2y** gave no desired product **7a-e**, suggesting that the reaction was

chemoselective towards silyl-substituted alkynes. To support our hypothesis, alkyne **2z** bearing diphenylethynyl and trimethylsilyl groups was used, and only trimethylsilyl-substituted *cis*-difunctionalization product **4w** was obtained in 46% yield, which convinced us of the chemoselectivity of this gold-catalysed transformation. Further expansion of the scope employing diazoniums **1b-d** bearing different structure skeletons and heterocycles gave desired products **5a-c** and **6a** in up to 60% yield. These results indicated that the reaction was well compatible with various diazoniums and highly selective towards silyl-substituted alkynes.

Table 1 Optimization of Reaction Conditions and Control Experiments^a



Entry	Au cat.	Photo cat.	Light	N ₂ /Air	Solvent	Yield [%] ^b
1	3a	-	blue ^c	N ₂	CH ₃ CN	71
2	3b	-	blue ^c	N ₂	CH ₃ CN	58
3	3c	-	blue ^c	N ₂	CH ₃ CN	75
4	3d	-	blue ^c	N ₂	CH ₃ CN	83
5	3e	-	blue ^c	N ₂	CH ₃ CN	n.d. ^d
6	3f	-	blue ^c	N ₂	CH ₃ CN	21
7	3g	-	blue ^c	N ₂	CH ₃ CN	trace
8	3h	-	blue ^c	N ₂	CH ₃ CN	n.d. ^d
9	3i	-	blue ^c	N ₂	CH ₃ CN	n.d. ^d
10	3j	-	blue ^c	N ₂	CH ₃ CN	n.d. ^d
11	-	-	blue ^c	N ₂	CH ₃ CN	n.d. ^d
12	3a	$\text{Ru}(\text{bpy})_3\text{Cl}_2$	blue ^c	N ₂	CH ₃ CN	9
13	3a	$\text{Ru}(\text{bpy})_3(\text{BF}_4)_2$	blue ^c	N ₂	CH ₃ CN	trace
14	3a	$\text{Ir}(\text{ppy})_3$	blue ^c	N ₂	CH ₃ CN	trace
15	3a	Rose Bengal	blue ^c	N ₂	CH ₃ CN	65
16	3a	-	dark	N ₂	CH ₃ CN	n.d. ^d
17	3a	-	blue ^c	N ₂	Toluene	trace
18	3a	-	blue ^c	N ₂	CH ₂ Cl ₂	trace
19	3a	-	blue ^c	N ₂	CH ₃ OH	trace
20	3a	-	blue ^c	Air	CH ₃ CN	35

^a Reaction conditions: treatment of **1a** (0.12 mmol), **2a** (0.10 mmol), gold catalyst **3a-j** (10 mol%) with or without photocatalyst (5 mol%) in 5 mL of solvent under N₂ at room temperature for 16 h. ^b Yield of **4a** was determined by ¹⁹F-NMR using fluorobenzene as internal standard. ^c Blue LEDs ($\lambda_{\text{max}} = 469 \text{ nm}$) was employed as light source. ^d n.d.: product formation could not be detected.

To provide insight on this visible light-mediated gold-catalysed *cis*-difunctionalization reaction, stoichiometric reactions were set up by treatment of aryl diazonium **1a** (0.10 mmol) with Ph_3PAuCl **3a** (0.10 mmol) under irradiation from 0 to



240 min. ^1H -NMR monitoring revealed that aryl diazonium **1a** consumed and new signals appeared gradually from 0 to 60 min, suggesting the formation of plausible intermediates (Fig. 1a). Irradiation for longer time gave slight decomposition of the plausible intermediates. These results were consistent to those observed by ^{31}P -NMR analysis, which indicated gradual appearance of new signals at 31.0, 44.2 and 45.3 ppm (Fig. 1b). The reaction mixtures were further treated with silyl-substituted alkyne **2a** (1.5 equiv.) for 60 min in dark, resulting in disappearance of the newly observed signals after irradiation and concomitant formation of the quinolizinium product **4a** (Fig. S3a-b in the ESI†). The yield of the product formed was monitored by ^{19}F -NMR analysis through addition of fluorobenzene as internal standard (Fig. S3c in the ESI†). In addition, regeneration of the Ph_3PAuCl **3a** could be recovered as precipitates from the reaction mixtures.

Table 2 Expansion of the substrate scope^{a,b}

Product	Yield (%)
4a	65%
4b	69%
4c	66%
4d	68%
4e	66%
4f	58%
4g	31%
4h	53%
4i	56%
4j	65%
4k	45%
4l	58%
4m	68%
4n	65%
4o	62%
4p	63%
4q	61%
4r	trace
4s	63%
4t	65%
4u	45%
5a	34%
5b	50%
5c	37%
6a	60%
4w	46%
2z	-
4v	not formed
7a	not formed
7b	not formed
7c	not formed
7d	not formed
7e	not formed

^a Reaction conditions: treatment of **1a-d** (0.60 mmol), **2a-z** (0.50 mmol) and **3a** (10 mol%) in 5 mL of CH_3CN under irradiation (blue LEDs) and N_2 at room temperature for 16 h. ^b Isolated yield.

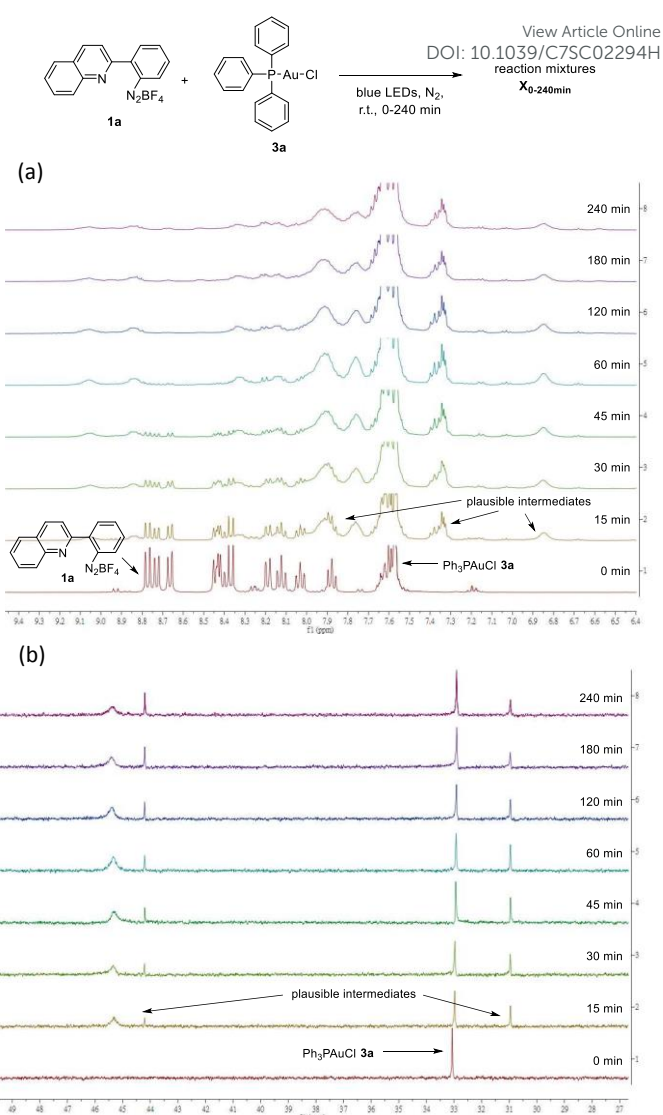


Fig. 1 (a) ^1H -NMR studies on reaction mixtures **X**_{0-240min} in CD_3CN ; (b) ^{31}P -NMR studies on reaction mixtures **X**_{0-240min} in CD_3CN .

Due to difficulties in isolation of the reaction intermediates, we sought to investigate the plausible Au(III) species through ESI-MS analysis by treatment of aryl diazonium **1a** (0.12 mmol) with Ph_3PAuCl **3a** (0.10 mmol) under irradiation for 1 h. Experimental results indicated that rather than the formation of **A** ($m/z = 204.0792$) by displacement of N_2 of **1a** in ESI-MS analysis, plausible Au(III) intermediates **B** ($m/z = 698.1014$) and **B'** ($m/z = 960.1910$) were found (Fig. 2a). Further treatment of the afforded reaction mixture **Y** with silyl-substituted alkyne **2a** (1.5 equiv.) in dark for 1 h afforded reaction mixture **Y'**. ESI-MS analysis of reaction mixture **Y'** revealed that no signal of **B** or **B'** was observed, and the signal of quinolizinium product **4a** appeared, suggesting that both **B** and **B'** were consumed and reacted with **2a** to form quinolizinium product **4a** (Fig. 2b). For detailed understanding of the plausible Au(III) intermediates **B** and **B'**, ESI-MS/MS analysis of species **B** (precursor ion $m/z = 698$) and **B'** (precursor ion $m/z = 910$) was conducted. Product ions phosphonium **B-I** ($m/z = 459.0483$) and Au(I) species **B-II** ($m/z = 466.1634$) were found in MS/MS analysis of species **B** (Fig. S4a in the ESI†). Formation of **B-I** was assumed to be ascribed to



reductive elimination of the Au(III) species **B**, which was previously reported as a feasible deactivation pathway of phosphine-supported aryl Au(III) complexes.¹⁵ In MS/MS analysis of species **B'**, product ions of **B** ($m/z = 698.1014$), **B-I** ($m/z = 466.1672$) and **B-II** ($m/z = 459.0518$) were found (Fig. S3b in the ESI[†]). Results suggested that species **B'** was composed of Au(III) species **B** and triphenylphosphine and presumably formed by possible transmetallation.¹⁶ Control experiment under the same reaction conditions without irradiation led to no formation of the Au(III) species **B**, **B'** or product **4a**, suggesting that light source was necessary for promotion of the Au(I)/Au(III) transformation in this reaction.

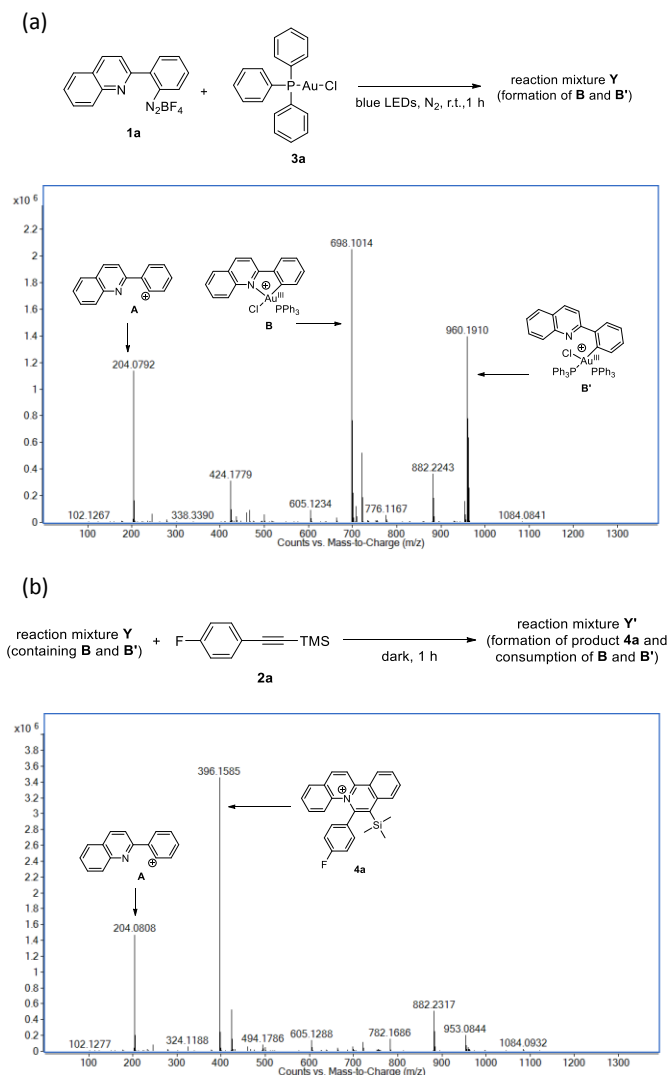


Fig. 2 (a) ESI-MS analysis of the reaction mixture **Y**; (b) ESI-MS analysis of the reaction mixture **Y'**.

To study the photosensitizer-free reaction conditions, we measured the UV/Vis absorption properties of aryl diazonium **1a** and Ph₃PAuCl **3a**. Spectroscopic analysis revealed that no absorption peak of Ph₃PAuCl **3a** was observed at $\lambda_{\text{abs}} > 395$ nm (Fig. S6 in the ESI[†]), indicating that Ph₃PAuCl **3a** might not be directly excited by the light source in this reaction which was consistent to literature works indicating that photosensitizer was necessary to initiate the reaction.³⁻⁵ On the contrary, a tail of the lowest energy absorption peak of aryl diazonium **1a** was

found at $\lambda_{\text{abs}} > 395$ nm (Fig. 3a), suggesting that aryl diazoniums could be firstly excited to initiate the reaction. To further support our hypothesis, we measured the difference of the fluorescence intensity before and after mixing Ph₃PAuCl **3a** (1 equiv.) with **1a**. Spectroscopic analysis indicated that the fluorescence of **1a** could be quenched ($I_q/I_0 = 0.68$) after addition of Ph₃PAuCl **3a**, providing strong evidence for electron transfer from Ph₃PAuCl **3a** to aryl diazonium **1a** under irradiation (Fig. 3b). In addition, the estimated excited state reduction potential (E^*_{red}) of aryl diazonium **1a** was 3.28 V, which was much more higher than the redox potential of Au(I)/Au(III) couple ($E_0 = 1.41$ V),¹⁸ indicating that the Ph₃PAuCl **3a** could be oxidized by the aryl diazonium **1a** in the first step of the reaction.

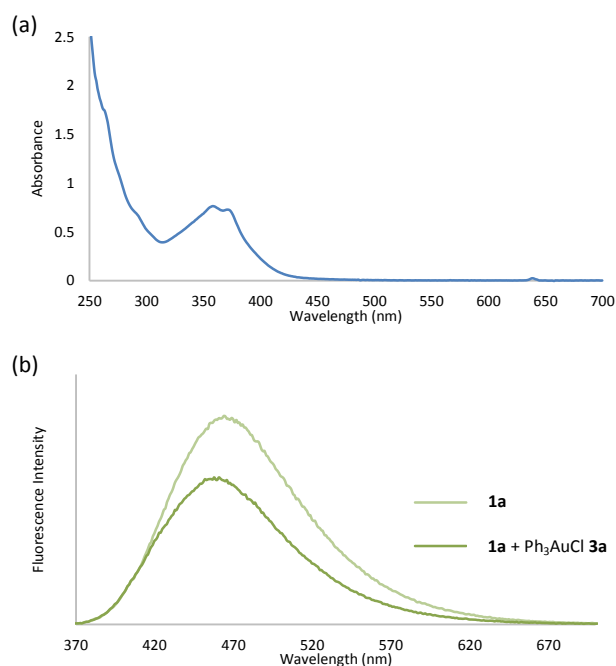


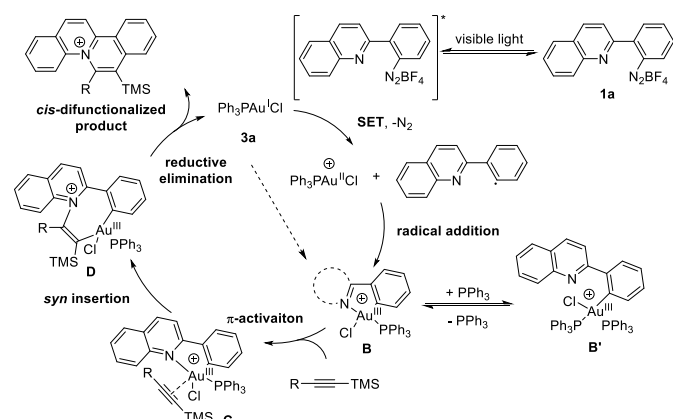
Fig. 3 (a) UV/Vis absorption spectrum of aryl diazonium **1a**; (b) fluorescence quenching of aryl diazonium **1a** with Ph₃PAuCl **3a**.

Based on the aforementioned experimental results, a reaction mechanism is proposed as below (Scheme 2). Under irradiation, the aryl diazonium compound is firstly excited and subsequently reduced by single electron transfer from Au(I) catalyst **3a** to form an aryl radical with the generation of a Au(II) species. The Au(II) species further recombines with the aryl radical to give Au(III) intermediate **B**. The oxidation and addition on Au(I) catalyst **3a** to form Au(III) intermediate **B** is also possible to be a concerted reaction pathway rather than a two-step process.^{6a} The reaction quantum yield was found to be 0.91 (less than 1), suggesting that the radical chain process was not prominent in this transformation. Then, silyl-substituted alkyne is activated by Au(III) intermediate **B** through π -activation to give species **C**. After that, the Au–N bond is regioselectively inserted by the π -activated alkyne to form *cis* vinyl gold species **D**. Then, reductive elimination provides quinolinium compound as the *cis*-difunctionalized product and regenerates the Au(I) catalyst **3a**.

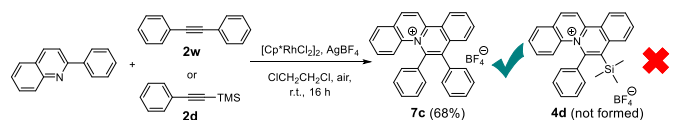
Pioneered by Cheng and co-workers,¹⁹ rhodium-catalysed C–H bond activation followed by annulation has been used as a



powerful tool for synthesis of disubstituted quinolizinium compounds. We sought to compare the newly developed approach of gold-catalysed *cis*-difunctionalization with the rhodium catalysis. Optimized reaction employing 2-phenylquinoline (0.1 mmol, 1 equiv.) with internal alkyne 1,2-diphenylethyne **2w** (0.1 mmol, 1 equiv.), [Cp*RhCl₂]₂ (5 mol%) and AgBF₄ (0.1 mmol, 1 equiv.) in 1,2-dichloroethane under open air at room temperature for 16 h afforded diphenyl-substituted quinolizinium **7c** in 68% yield. However, when 1-phenyl-2-trimethylsilylacetylene **2d** was employed as substrate, no desired product **4d** was formed. To our knowledge, the present photosensitizer-free visible light-mediated gold-catalysed alkyne *cis*-difunctionalization is the first example for highly regioselective synthesis of silyl-substituted quinolizinium compounds.



Scheme 2 Proposed reaction mechanism.



Scheme 3 Rhodium-catalysed synthesis of quinolizinium compounds.

X-ray crystal structure analysis revealed a twisted conformation of quinolizinium **4b**, with a torsion angle of 107.84° (C1-C2-C18-C19), suggesting that the molecule could be divided into two parts: a slightly distorted planar quinolizinium moiety and a phenyl moiety. This twisted structure suggested that the two moieties should be weakly coupled conjugatively.

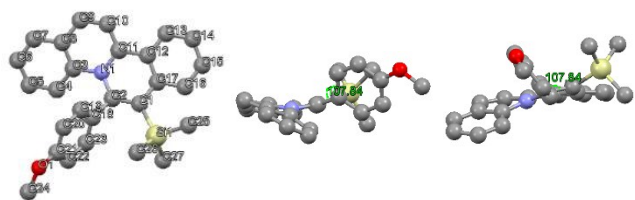


Fig. 4 X-ray crystal structure of **4b** (front view, left view and vertical view).

After synthesis of the new silyl-substituted quinolizinium compounds, we moved on to study their absorption and emission properties (Table 3). Interestingly, these compounds possessed lowest energy absorption maximum at $\lambda_{\text{abs}} > 395$ nm, full color tunable emission properties ($\lambda_{\text{em}} = 450$ to 640 nm) in visible light region and large Stokes shifts (up to 6797 cm⁻¹) with

quantum yield up to 0.59. Incorporation of electron-donating groups at the *para*-position of phenyl moiety or introduction of π -excessive heteroaromatics resulted in bathochromic shifts of the emission properties. Further bathochromic shifts were observed by introduction of electron-withdrawing ester group on the quinolizinium moiety. Substituents bearing heavy atoms (Cl, Br, I) led to lower quantum yields. A positive solvatochromism was found in compound **4b**, which indicated an increase of dipole moment of the excited state compared to its ground state (Fig. S8 in the ESI[†]). An unexpectedly low quantum yield of **5a** (0.02) bearing a dimethylamine substituent was observed, in which the fluorescence was proposed to be quenched by the amine group via intramolecular photo-induced electron transfer (PeT). Cyclic voltammetry (CV) experiments indicated a quasireversible oxidation couple at +1.08 V (vs SCE) of **5a** which was originated from the presence of amine group and no similar peak was found in **5c** (ESI[†]). Protonation of the amine group by measuring the emission in HCl/NaOH buffer (pH changing from 7 to 1) gave a ≥ 100 fold enhancement of the emission intensity at shorter wavelength ($\lambda_{\text{em}} = 436$ nm) which supported our hypothesis (Fig. S9 in the ESI[†]).

Table 3 Photophysical properties of quinolizinium compounds **4a-q**, **5a-c**

Cpd.	Absorption maximum λ_{abs} (nm) (ϵ (10 ⁴ dm ³ mol ⁻¹ cm ⁻¹))	Emission maximum λ_{em} (nm)	Stokes shift (cm ⁻¹)	Quantum yield Φ_F^b
4a	423 (1.39)	495	3439	0.49
4b	430 (1.14)	569	5681	0.17
4c	428 (1.10)	507	3640	0.44
4d	423 (1.45)	491	3275	0.44
4e	424 (1.62)	494	3342	0.37
4f	422 (0.95)	493	3413	0.16
4g	424 (1.00)	493	3301	0.03
4h	423 (1.06)	480	2807	0.28
4i	417 (0.75)	484	3320	0.44
4j	420 (1.30)	479	2933	0.28
4k	420 (1.17)	479	2933	0.34
4l	419 (1.23)	476	2858	0.24
4m	423 (1.45)	506	3878	0.18
4n	424 (1.68)	508	3900	0.16
4o	428 (1.43)	547	5363	0.02
4p	421 (1.50)	511	4183	0.11
4q	423 (1.80)	511	4071	0.16
4s	446 (0.79)	640	6797	0.01
4t	446 (1.05)	557	4468	0.08
4u	424 (1.42)	494	3342	0.41
4w	427 (1.05)	555	5401	0.07
5a	397 (1.74)	495	4987	0.02
5b	405 (1.23)	504	4850	0.30
5c	401 (1.09)	450	2840	0.59

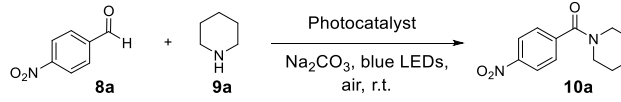
^a Absorption and emission properties were measured in CH₂Cl₂ at the concentration of 1×10^{-5} M. ^b Quantum yields were measured using fluorescein ($\Phi_F = 0.95$ in 0.1 N NaOH buffer) as standard.



For detailed investigation of the SPFR of the quinolinizinium compounds, compound **4d** was subjected to TDDFT calculation. Results reveal that the lowest energy absorption band at 435 nm is originated from HOMO→LUMO. HOMO is composed of π orbital of quinolinizinium and phenyl ring whereas LUMO is composed of π^* of quinolinizinium ring. The low energy absorption band can be assigned as admixture of $\pi \rightarrow \pi^*$ transition within the quinolinizinium ring and $\pi \rightarrow \pi^*$ transition from phenyl to quinolinizinium ring. Hence, bathochromic shifts were observed by introduction of ester group at C9 (LUMO was dominant) and introduction of electron-donating groups at C21 (HOMO was partially dominant).

In line with our interest in amide synthesis,²⁰ we envisioned that the newly developed quinolinizinium fluorophores could be utilized as photocatalysts for photooxidative amidation of aldehydes and secondary amines. We first investigated the catalytic activities by treatment of 4-nitrobenzaldehyde **8a** (0.1 mmol, 1 equiv.), piperidine **9a** (0.2 mmol, 2 equiv.), Na₂CO₃ (0.2 mmol, 2 equiv.) and selected photocatalysts (5 mol%) in CH₃CN under irradiation (blue LEDs) and air for 16 h. Interestingly, the catalytic activities of quinoliniziniums were comparable or even better than the currently used photocatalysts. The reaction was optimized using **4e** as photocatalyst to afford amide **10a** in 86% yield after 48 h. Expansion of the scope employing different aldehydes and secondary amines gave amides **10b-g** in up to 84% yield (Table 5). Further investigations revealed that the quinolinizinium compounds possessed tunable and high excited state reduction potential ($E^*_{\text{red}} = 1.97$ to 2.23 V), which were comparable to the well-known photocatalyst 9-mesityl-10-methylacridinium [Acr⁺-Mes](BF₄) developed by Fukuzumi.²¹ To our knowledge, this is the first example employing quinoliniziniums as photocatalysts for visible light-mediated photoredox catalysis.

Table 4 Photooxidative amidation using quinolinizinium compounds as photocatalysts^a



Entry	Photo cat.	E^*_{red} (V)	Time (h)	Yield [%] ^b
1	4a	1.99	16	53
2	4b	1.97	16	50
3	4e	2.21	16	61
4	4f	2.22	16	59
5	4j	2.24	16	52
6	4p	2.07	16	53
7	Eosin Y	1.23 ^c	16	48
8	Fluorescein	1.25 ^c	16	47
9	Rose Bengal	1.18 ^c	16	32
10	[Acr ⁺ -Mes](BF ₄)	2.08 ^c	16	44
11	4e	2.21	48	86
12 ^d	4e	2.21	48	71 ^e

^a Reaction conditions: treatment of **8a** (0.1 mmol, 1 equiv.), **9a** (0.2 mmol, 2 equiv.), Na₂CO₃ (0.2 mmol, 2 equiv.) and photocatalyst (5 mol%) in 5 mL of CH₃CN under blue LEDs and air at room temperature. ^b Yield was determined by ¹H-NMR using 1,3,5-trimethoxybenzene as internal standard. ^c E^*_{red} refers to ref. 9a and literatures cited there. ^d Reaction was performed by treatment of **8a** (1 mmol, 1 equiv.), **9a** (2 mmol, 2 equiv.), Na₂CO₃ (2 mmol, 2 equiv.) and photocatalyst (5 mol%) in 5 mL of CH₃CN under blue LEDs and air at room temperature. ^e Isolated yield.

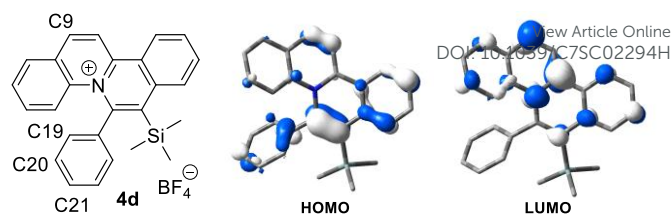
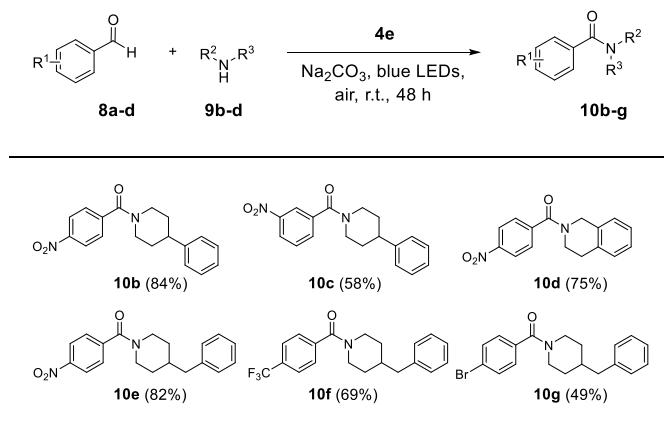


Fig. 5 HOMO and LUMO diagrams of **4d**.

Table 5 Photooxidative amidation of aldehydes with secondary amines^a



^a Reaction conditions: treatment of **8a-d** (0.1 mmol, 1 equiv.), **9b-d** (0.2 mmol, 2 equiv.), Na₂CO₃ (0.2 mmol, 2 equiv.) and photocatalyst **4e** (5 mol%) in 5 mL of CH₃CN under blue LEDs and air at room temperature for 48 h. ^b Isolated yield.

The feasibility in cellular imaging was demonstrated by incubation of HeLa cells with 2 μ M of the fluorescent quinolinizinium compounds **4a-b**, **d**, **f**, **h**, **i-o**, **s-t**, **w** and **5c**, respectively (experimental details in the ESI[†]). Confocal fluorescence microscopic images revealed that the quinoliniziniums were selectively localized in cytoplasm with no transportation into the nucleus, which was different from the known examples of quinoliniziniums.²² Compound **5c** and **4l** were chosen for colocalization studies to track the subcellular localization. Compound **5c** was specifically localized in mitochondria (Fig. 6a-c), which could be attributed to the presence of the positively charged quinolinizinium skeleton, directing it towards the mitochondria membrane with -180 mV potential. Interestingly, apart from localization in mitochondria, compound **4l** bearing a nitro substituent localized mainly in lysosome and partially in late endosome (Fig. 6d-i). The subcellular localization of the quinoliniziniums could be switched by simply modifying the substituents, and these compounds would be amenable for the design of specific molecular probes for individual organelle imaging.

Conclusions

In summary, we have developed the first photosensitizer-free visible light-mediated gold-catalysed *cis*-difunctionalization reaction with high chemoselectivity and excellent regioselectivity for modular synthesis of a series of silyl-substituted quinolinizinium compounds. Control experiments as well as a combination of NMR, ESI-MS and spectroscopic analysis indicate a plausible visible light-mediated Au(I)/Au(III)



catalytic transformation involving a regioselective *syn* insertion of silyl-substituted alkynes. Additionally, we have studied applications of the newly synthesized silyl-substituted quinolizinium compounds in photooxidative amidation and cellular imaging. The efficient modular synthesis and unique photophysical properties of the quinolizinium compounds would open up a new direction in gold catalysis, photoredox catalysis and molecular imaging.

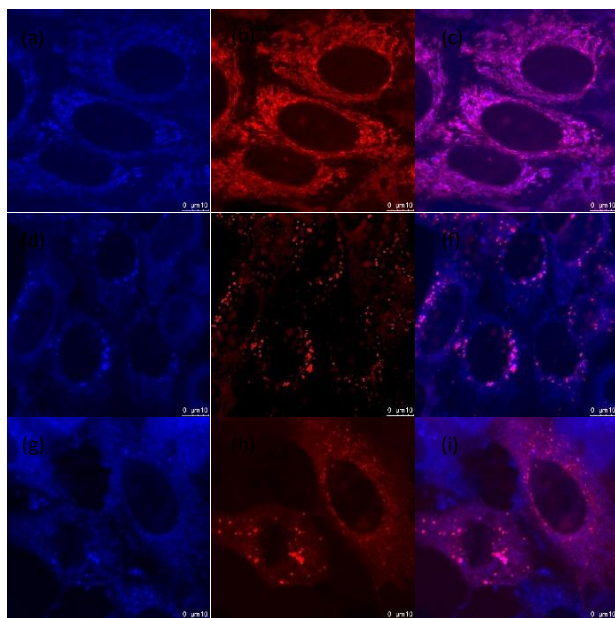


Fig. 6 Confocal fluorescence microscopic images of HeLa cells. (a) sub-cellular localization of **5c**; (b) subcellular localization of MitoTracker® Red; (c) merged images of (a) and (b); (d) subcellular localization of **4l**; (e) subcellular localization of LysoTracker® Deep Red; (f) merged images of (d) and (e); (g) subcellular localization of **4l**; (h) subcellular localization of mRFP-Rab7; (i) merged images of (g) and (h).

Acknowledgements

We are grateful for the financial support of National Natural Science Foundation of China (21272198), Hong Kong Research Grants Council (PolyU 153031/14P, 153001/17P, X-ray diffractometer-PolyU11/CRF/13E), State Key Laboratory of Chirosciences and Department of Applied Biology and Chemical Technology. We thank Prof. K.-Y. Wong for facilitating the project by providing access to Bioanalytical Systems (BAS) for cyclic voltammetry ex-periments and Prof. Z. Zhou and Dr. W. T.-K. Chan for X-ray crystallographic analysis.

Notes and references

- 1 a) A. S. K. Hashmi and G. J. Hutchings, *Angew. Chem. Int. Ed.*, 2006, **45**, 7896; b) A. S. K. Hashmi, *Chem. Rev.*, 2007, **107**, 3180; c) Z. Li, C. Brouwer and C. He, *Chem. Rev.*, 2008, **108**, 3239; d) A. Arcadi, *Chem. Rev.*, 2008, **108**, 3266; e) E. Jiménez-Núñez and A. M. Echavarren, *Chem. Rev.*, 2008, **108**, 3326; f) D. J. Gorin, B. D. Sherry and F. D. Toste, *Chem. Rev.*, 2008, **108**, 3351; g) N. Krause and C. Winter, *Chem. Rev.*, 2011, **111**, 1994; h) H.-S. Yeom and S. Shin, *Acc. Chem. Res.*, 2014, **47**, 966; i) Z.

- Zheng, Z. Wang, Y. Wang and L. Zhang, *Chem. Soc. Rev.*, 2016, **45**, 4448; j) A. M. Asiri and A. S. K. Hashmi, *Chem. Soc. Rev.*, 2016, **45**, 4471; k) W. Zi and F. D. Toste, *Chem. Soc. Rev.*, 2016, **45**, 4567.
- 2 a) M. N. Hopkinson, A. D. Gee and V. Gouverneur *Chem. - Eur. J.* 2011, **17**, 8248; b) H. A. Wegner and M. Auzias, *Angew. Chem. Int. Ed.*, 2011, **50**, 8236.
- 3 a) M. N. Hopkinson, A. Tlahuext-Aca and F. Glorius, *Acc. Chem. Res.*, 2016, **49**, 2261; b) B. Sahoo, M. N. Hopkinson and F. Glorius, *J. Am. Chem. Soc.*, 2013, **135**, 5505; c) M. N. Hopkinson, B. Sahoo and F. Glorius, *Adv. Synth. Catal.*, 2014, **356**, 2794; d) A. Tlahuext-Aca, M. N. Hopkinson, B. Sahoo and F. Glorius, *Chem. Sci.*, 2016, **7**, 89; e) A. Tlahuext-Aca, M. N. Hopkinson, R. A. Garza-Sanchez and F. Glorius, *Chem. - Eur. J.*, 2016, **22**, 5909.
- 4 a) M. D. Levin, S. Kim and F. D. Toste, *ACS Cent. Sci.*, 2016, **2**, 293; b) X.-Z. Shu, M. Zhang, Y. He, H. Frei and F. D. Toste, *J. Am. Chem. Soc.*, 2014, **136**, 5844; c) Y. He, H. Wu and F. D. Toste, *Chem. Sci.*, 2015, **6**, 1194; d) S. Kim, J. Rojas-Martinab and F. D. Toste, *Chem. Sci.*, 2016, **7**, 85.
- 5 a) D. V. Patil, H. Yun and S. Shin, *Adv. Synth. Catal.*, 2015, **357**, 2622; b) J. Um, H. Yun and S. Shin, *Org. Lett.*, 2016, **18**, 484; c) Z. Xia, O. Khaled, V. Mouriès-Mansuy, C. Ollivier and L. Fensterbank, *J. Org. Chem.*, 2016, **81**, 7182; d) T. Cornilleau, P. Hermange and E. Fouquet, *Chem. Commun.*, 2016, **52**, 10040; e) V. Gauchot and A.-L. Lee, *Chem. Commun.*, 2016, **52**, 10163; f) V. Gauchot, D. R. Sutherland and A.-L. Lee, *Chem. Sci.*, 2017, **8**, 2885.
- 6 a) L. Huang, M. Rudolph, F. Rominger and A. S. K. Hashmi, *Angew. Chem. Int. Ed.*, 2016, **55**, 4808; b) S. Witzel, J. Xie, M. Rudolph and A. S. K. Hashmi, *Adv. Synth. Catal.*, 2017, **359**, 1522.
- 7 a) M. Joost, A. Amgoune and D. Bourissou, *Angew. Chem. Int. Ed.*, 2015, **54**, 15022; b) F. Rekhroukh, R. Brousses, A. Amgoune and D. Bourissou, *Angew. Chem. Int. Ed.*, 2015, **54**, 1266; c) F. Rekhroukh, C. Blons, L. Estévez, S. Mallet-Ladeira, K. Miqueu, A. Amgoune and D. Bourissou, *Chem. Sci.*, 2017, **8**, 4539; d) C. Gryparis, M. Kidonakis and M. Stratakis, *Org. Lett.*, 2013, **15**, 6038; e) C. Gryparis and M. Stratakis, *Org. Lett.*, 2014, **16**, 1430.
- 8 K. D. Hesp and M. Stradiotto, *J. Am. Chem. Soc.*, 2010, **132**, 18026.
- 9 a) N. A. Romero and D. A. Nicewicz, *Chem. Rev.*, 2016, **116**, 10075; b) X. Li, X. Gao, W. Shi and H. Ma, *Chem. Rev.*, 2014, **114**, 590; c) H. Uoyama, K. Goushi, K. Shizu, H. Nomura and C. Adachi *Nature*, 2012, **492**, 234; d) G. J. Hedley, A. Ruseckas and I. D. W. Samuel, *Chem. Rev.*, 2017, **117**, 796.
- 10 a) H. Kobayashi, M. Ogawa, R. Alford, P. L. Choyke and Y. Urano, *Chem. Rev.*, 2010, **110**, 2620; b) A. Loudet and K. Burgess, *Chem. Rev.*, 2007, **107**, 4891; c) E. Kim, Y. Lee, S. Lee and S. B. Park, *Acc. Chem. Res.*, 2015, **48**, 538.
- 11 a) Z. Xu and L. Xu, *Chem. Commun.*, 2016, **52**, 1094; b) W. Xu, Z. Zeng, J. H. Jiang, Y. T. Chang and L. Yuan, *Angew. Chem. Int. Ed.*, 2016, **55**, 13658.
- 12 a) G. Anton and I. Heiko, *Synlett*, 2016, **27**, 1775; b) D. Sucunza, A. M. Cuadro, J. Alvarez-Builla and J. J. Vaquero, *J. Org. Chem.*, 2016, **81**, 10126; c) A. Granzhan, H. Ihmels and G. Viola, *J. Am. Chem. Soc.*, 2007, **129**, 1254.
- 13 A. Barbafrina, A. M. melia, L. Latterini, G. G. Aloisi and F. Elisei, *J. Phys. Chem. A*, 2009, **113**, 14514.
- 14 a) V. K.-Y. Lo, Y. Liu, M.-K. Wong and C.-M. Che, *Org. Lett.*, 2006, **8**, 1529; b) H.-M. Ko, K. K.-Y. Kung, J.-F. Cui and M.-K. Wong, *Chem. Commun.*, 2013, **49**, 8869; c) J.-F. Cui, H.-M. Ko, K.-P. Shing, J.-R. Deng, N. C.-H. Lai and M.-K. Wong, *Angew. Chem. Int. Ed.*, 2017, **56**, 3074.
- 15 H. Kawai, W. J. Wolf, A. G. DiPasquale, M. S. Winston and F. D. Toste, *J. Am. Chem. Soc.*, 2016, **138**, 587.



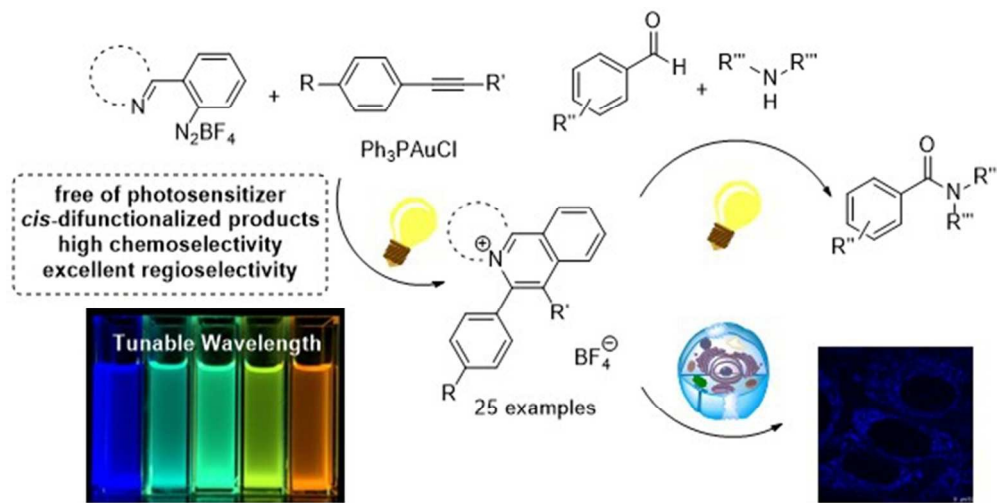
ARTICLE

Journal Name

- 16 W. J. Wolf, M. S. Winston and F. D. Toste, *Nat. Chem.*, 2014, **6**, 159.
- 17 M. S. Winston, W. J. Wolf and F. D. Toste, *J. Am. Chem. Soc.*, 2014, **136**, 7777.
- 18 S. G. Bratsch, *J. Phys. Chem. Ref. Data*, 1989, **18**, 1.
- 19 a) C.-Z. Luo, P. Gandeepan and C.-H. Cheng, *Chem. Commun.*, 2013, **49**, 8528; b) C.-Z. Luo, P. Gandeepan, J. Jayakumar, K. Parthasarathy, Y.-W. Chang and C.-H. Cheng, *Chem. - Eur. J.*, 2013, **19**, 14181; c) C.-Z. Luo, P. Gandeepan, Y.-C. Wu, C.-H. Tsai and C.-H. Cheng, *ACS Catal.*, 2015, **5**, 4837.
- 20 a) W.-K. Chan, C.-M. Ho, M.-K. Wong and C.-M. Che, *J. Am. Chem. Soc.*, 2006, **128**, 14796; b) A. O.-Y. Chan, C.-M. Ho, H.-C. Chong, Y.-C. Leung, J.-S. Huang, M.-K. Wong and C.-M. Che, *J. Am. Chem. Soc.*, 2012, **134**, 2589; c) G.-L. Li, K. K.-Y.; Kung and M.-K. Wong, *Chem. Commun.*, 2012, **48**, 4112; d) F. K.-C. Leung, J.-F. Cui, T.-W. Hui, K. K.-Y. Kung and M.-K. Wong, *Asian J. Org. Chem.*, 2015, **4**, 533.
- 21 S. Fukuzumi, H. Kotani, K. Ohkubo, S. Ogo, N. V. Tkachenko and H. Lemmetyinen, *J. Am. Chem. Soc.*, 2004, **126**, 1600.
- 22 a) R. Bortolozzi, H. Ihmels, L. Thomas, M. Tian and G. Viola, *Chem. - Eur. J.*, 2013, **19**, 8736; b) A. C. Shaikh, D. S. Ranade, P. R. Rajamohanan, P. P. Kulkarni and N. T. Patil, *Angew. Chem. Int. Ed.*, 2017, **56**, 757.

View Article Online
DOI: 10.1039/C7SC02294H





164x82mm (96 x 96 DPI)

